

An analysis of satellite planar configurations around the MW and M31: singling out new high quality planes

Isabel M. Santos-Santos^{1,2*}, Rosa Domínguez-Tenreiro¹, Marcel S. Pawlowski³

¹*Departamento de Física Teórica, Universidad Autónoma de Madrid, 28049 Cantoblanco, Madrid, Spain & CIAFF*

²*Department of Physics and Astronomy, University of Victoria, Victoria, BC, Canada V8P 5C2*

³*Leibniz-Institute für Astrophysik Potsdam, An der Sternwarte 16, D-14482 Potsdam, Germany*

Accepted XXXX . Received XXXX; in original form XXXX

ABSTRACT

We present a detailed characterization of planes of satellites in the Milky Way (MW) and M31 systems. To this end we introduce an extension to the ‘4-galaxy-normal density plot’ method (Pawlowski et al. 2013), by which plot over-densities signal the normal direction to predominant planes of satellites within a given sample. For a given over-density, the extension provides a *collection* of planes, each including a different number of objects N_{sat} . We apply this method to the position data of confirmed MW and M31 satellites and quantify the quality of planes through the outputs of a Tensor of Inertia plane-fitting technique. Plane quality is quantified in terms of population (N_{sat}) and flattening (the short-to-long axis ratio c/a or the rms thickness normal to the plane). Therefore, planes with the same population or flattening can be compared with each other allowing us to single-out best-quality planes.

For the first time, we study the second-most predominant planar configuration of satellites in M31, singling out a plane with 18 satellite members that shows a quality comparable to the Great Plane of Andromeda (GPoA, with $N_{\text{sat}} = 19$) despite it being more affected by distance uncertainties. This structure is viewed nearly face-on from the MW and is approximately normal to the GPoA.

Overall, we find planes of satellites around the MW and M31 with higher qualities than those previously reported with a given N_{sat} . We also show that mass plays no role in determining a satellite’s membership or not to the respective best-quality planes.

Key words: galaxies: dwarf - Local Group - kinematics and dynamics methods: statistical cosmology: theory

1 INTRODUCTION

The known objects surrounding the Milky Way (MW) show an anisotropic spatial distribution. Lynden-Bell (1976) and Kunkel & Demers (1976) were the first to notice that dSphs Sculptor, Draco, Ursa Minor and globular cluster Palomar 13, apparently lied on the orbital plane of the Magellanic stream, therefore polar to the Galaxy. Soon after, Fornax, Leo I, Leo II, Sextans, Phoenix and some classified as ‘young halo’ globular clusters, were also found to participate of this “great circle” (Lynden-Bell 1982; Majewski 1994; Fusi Pecci et al. 1995). The existence of a “plane of satellites” in the MW was finally ratified when measuring the very flattened distribution of the 11 classical satellites as compared to isotropy (Kroupa et al. 2005; Metz et al. 2007). In our neighboring galactic

system Andromeda (M31), the first studies by Grebel et al. (1999) and Koch & Grebel (2006) on the then-known $\lesssim 15$ dwarf galaxies within ~ 500 kpc distance, found that the subsample of dSph/dE type dwarfs also lied near a “great circle”. This spatial anisotropy was emphasized by the skewness of M31 dwarfs in the direction to the MW (McConnachie & Irwin 2006). More recently, the addition to the picture of newly discovered faint satellites thanks to surveys like SDSS (York et al. 2000) or PAndAS (McConnachie et al. 2009), and an increased quality of distance measurements, has only enhanced the significance of the planar structures noted in the MW and M31 (Metz et al. 2009; Kroupa et al. 2010; Ibata et al. 2013; Conn et al. 2013; Pawlowski et al. 2013; Pawlowski & Kroupa 2014; Pawlowski et al. 2015). In addition, a richer census of young halo globular clusters and several stellar/gaseous streams have been shown to also align with the MW satellites (Keller et al. 2012; Pawlowski et al. 2012). Finally, apart from the MW and M31, there are claims for a planar distribution of satellites in the nearby Centaurus A Group of galaxies (Tully et al. 2015), further sup-

* E-mail: isabelm.santos@uam.es

ported by discoveries of new dwarfs and better distance estimates (Müller et al. 2016, 2018).

In the last years, the quantification of such planar alignments has gained increasing importance in order to unambiguously define the observed structures in terms of their orientation and characteristics. These quantifications have demanded increasingly more sophisticated methods that make use of the three-dimensional position data as well as statistical approaches to overcome measurement uncertainties or avoid spurious effects coming from working with a small sample number.

Specifically, Koch & Grebel (2006) used an error-weighted orthogonal distance regression accompanied by bootstrapped tests, to reliably determine a robust solution for estimating best-fit planes. They fitted a plane to all possible subsamples of M31 satellites involving 3 to 15 members and projected the resulting normal vectors on a sphere. With the density distribution of normals they found an estimation of the normal direction to the broad planar distribution defined by the satellites' positions. Metz et al. (2007, 2009) used instead the Tensor of Inertia plane-fitting method taking into account distance uncertainties. More recently, Pawlowski et al. (2013) combined the previous efforts and presented a new statistical method to define the direction of predominant plane-like spatial distributions of satellites within a given sample: the '4-galaxy-normal density plot' method, consisting of a planar fit to every combination of 4 satellites. From its application to the confirmed satellites within 300 kpc in the MW and M31 they obtained the normal direction to one predominant planar alignment of satellites in each galactic system. In this way, the so-called "VPOS-3" (Vast Polar Structure) and "GPoA" (Great Plane of Andromeda) planes were defined, consisting of 24 and 19 satellites respectively. These planes have been considered so far to be the most relevant satellite planar configurations in the MW and M31, and have been used as a benchmark against which to test the alignment of the newest (unclassified) objects discovered (Pawlowski & Kroupa 2014; Pawlowski et al. 2015). However, an identification of the "best" planes of satellites in the MW and M31 formed by a variable number of members is still lacking. This identification demands an analysis of how the *quality* of these planes changes with the number of satellites included.

The purpose of this paper is to present a more detailed quantification and characterization of the plane-like spatial structures in the MW and M31 satellite systems. This is an important issue and, additionally, it will provide a reference with which to compare results from numerical simulations analyses (Santos-Santos in prep.). We will focus on the positions of satellites, which for the MW have error bars much smaller than those of kinematic data. We note, however, that complementary, relevant information to satellite planar alignments comes from kinematic data. Indeed, recent proper motions for MW satellites measured with GAIA (Gaia Collaboration et al. 2018) suggest that a non-negligible fraction of them are orbiting within the VPOS (Fritz et al. 2018). For M31 satellites just line-of-sight velocities (Ibata et al. 2013) are currently available.

In this work we build on the results of Pawlowski et al. (2013) and develop an extension to their '4-galaxy-normal density plot' method that enables a deeper study on cataloguing and quality analyses of planes of satellites. In particular, for each predominant planar configuration of satellites in the MW and M31 found with the previous method, we yield a collection of planes of satellites with an increasing number of members, and identify the highest-quality planes in terms of the Tensor of Inertia parameters. In particular, a plane's quality is quantified in terms of its population (N_{sat}) and flattening (the concentration ellipsoid short-to-long axis ratio c/a or, equivalently, the r.m.s. thickness normal to the plane; CRAMR

1999). Quality of planes with the same population or flattening can be compared with each other, allowing to single-out best quality planes with the same N_{sat} or c/a values.

The paper is organized as follows. In Sec. 2 we present the sample and dataset of MW and M31 satellites studied. In Sec. 3 we thoroughly describe our methodology. Secs. 4.1 and 4.2 show the results of our quality analysis for planes in the MW and M31, respectively. Finally Sec. 5 summarizes our conclusions.

2 MW AND M31 DATA

In this study we use the same satellite samples as in Pawlowski et al. (2013), consisting of 27 and 34 satellites for the MW and M31, respectively. These are the confirmed satellites within 300 kpc from their hosts, according to the McConnachie (2012) "Nearby dwarf galaxy database"¹ as on the 17th of June 2013. Therefore Canis Major and AXXVII are considered here as dwarf galaxies although their nature is debated (see Momany et al. 2004; Martínez-Delgado et al. 2005; Mateu et al. 2009; Martin et al. 2016). Most probable satellite position values and their corresponding Gaussian width uncertainties in the radial Sun - satellite distance have been taken from this database, as summarized in Pawlowski et al. (2013) Table 2. The sample analyzed in this paper considers all the classical plus SDSS satellites. We will ignore the more recently discovered dwarf galaxy candidates (see for example Bechtol et al. 2015; Koposov et al. 2015) which originate from a wide variety of sources/surveys, for the sake of consistency with Pawlowski et al. (2013), and for simplicity as far as comparisons are concerned (see also Pawlowski 2016).²

The different observational planes of satellites claimed in the literature which we will compare to (defined considering the same sample of satellites) are listed in Table 1. This Table shows the properties (see next section for property definitions) of these observed planes as reported by the most up-to-date studies. For the MW these planes are: the so-called classical (i.e., the 11 most luminous MW satellites, see Metz et al. 2007), the VPOSall (Pawlowski et al. 2013, defined by all the 27 confirmed satellites within 300 kpc), and the VPOS-3 (Pawlowski et al. 2013, defined by 24 out of 27 of the VPOSall satellites). For M31, there is the plane of satellites noted by Ibata et al. (2013) and Conn et al. (2013) with the PAndAS survey, which we will consider with 14 satellites (as analyzed in Pawlowski et al. 2013, hereafter the 'Ibata-Conn-14' plane)³, and the so-called GPoA (Pawlowski et al. 2013), with 19 members (the 14 of the 'Ibata-Conn-14' plane plus 5 more). We note that other planes of satellites in the Local Group have been suggested in Shaya & Tully (2013), but under the consideration of a different initial sample of satellites than that used here. In particular, they define 4 satellite planes (2 in the MW and 2 in M31). The so-called "plane 1" includes a majority of satellites that participate in the GPoA, while "plane 4" is basically a reduced version of the classical plane in the MW plus dwarf galaxy Phoenix.

¹ http://www.astro.uvic.ca/~alan/Nearby_Dwarf_Database_files/NearbyGalaxies.dat

² As shown in Pawlowski & Kroupa (2014); Pawlowski et al. (2015), the majority of the recently discovered dwarf galaxy candidates in the MW align with the VPOS. While their consideration in our analysis would produce different results to those presented here, the same conclusions remain regarding the general quality behaviour of the MW planar structures.

³ Pawlowski et al. (2013) did not consider AXVI as a satellite because it is further than 300 kpc away.

3 SEARCHING FOR PREDOMINANT PLANAR CONFIGURATIONS AND PLANE QUALITY ANALYSIS

Our method to find planar structures and assess their quality consists of 2 parts. The first part follows the ‘4-galaxy-normal density plots’ method described in Pawlowski et al. (2013). This technique checks if there is a subsample of a given satellite sample that defines a dominant planar arrangement in terms of the outputs of the standard Tensor of Inertia (ToI) plane-fitting technique (see Metz et al. 2007; Pawlowski et al. 2013), based on an orthogonal-distance regression. In terms of the corresponding concentration ellipsoid, planes are characterized by:

- N_{sat} : the number of satellites in the subsample;
- \vec{n} , the normal to the best fitting plane;
- c/a : the ellipsoid short-to-long axis ratio;
- b/a : the ellipsoid intermediate-to-long axis ratio;
- ΔRMS : the root-mean-square thickness perpendicular to the best-fitting plane;
- D_{cg} : the distance from the center-of-mass of the main galaxy to the plane.

These outputs are used to quantify the quality of planes. To begin with, a planar configuration must be flattened (i.e., low c/a), and, as opposed to filamentary, it also requires $b/a \sim 1$ for an oblate distribution. High quality planes are those with a high N_{sat} , and a low c/a and ΔRMS , meaning they are populated and thin (plane quality as understood in this work will be specified in more detail at the end of the next section). Moreover, the plane normal \vec{n} determines the plane direction, for example in view of Aitoff projection purposes. Finally, a low D_{cg} means that the plane passes near the main galaxy’s center; a characteristic to be requested if the planes are expected to live within a potential making them dynamically stable, assuming that the host galaxy center is close to the center of the system’s gravitational potential well.

The second part of our methodology, which is the focus of this paper, is an extension to the 4-galaxy-normal density plot method, consisting of a quality analysis of the predominant planar arrangements found.

3.1 4-galaxy-normal density plot method

This method was presented in Sec. 2.4 of Pawlowski et al. (2013). We briefly summarize it and mention the procedure particularities followed in this study.

(i) A plane is fitted to every combination of four⁴ satellites’ positions, using the ToI technique. The resultant normal vector (i.e. 4-galaxy-normal) and corresponding plane parameters are stored. To account for distance uncertainties, this step is repeated 100 times using 100 random positions per satellite, calculated using their corresponding radial distance uncertainties.

(ii) All the 4-galaxy-normals (from all 100 realizations) are projected on a regularly-binned sphere, assuming a Galactocentric coordinate system such that the MW’s disc spin vector points towards

⁴ Three points always define a plane, not allowing any quantification of plane thickness. Therefore 4 is the lowest possible amount to take into consideration under the condition of making the number of combinations as high as possible. This is important in order to analyze sets of satellites consisting of a low number of objects, as is frequently the case in satellite populations.

the south pole. A density map (i.e. 2D-histogram) is drawn from the projections, where each normal has been weighted by $\log\left(\frac{a+b}{c}\right)$ to emphasize planar-like spatial distributions. The over-density regions in these density maps (i.e. regions of 4-galaxy-normal accumulation) therefore signal the normal direction to a dominant planar space-configuration. Satellites contributing 4-galaxy-normals to a given over-density are likely members of such a dominant plane. As opposite normal vectors indicate the same plane, density maps in this study are shown through Aitoff spherical projection diagrams in Galactic coordinates (longitude l , latitude b) within the $l = [-90^\circ, +90^\circ]$ interval.

(iii) We order bins by density value. The main over-density region is identified around the highest value bin. Subsequent over-densities are identified by selecting the next bin, in order of decreasing density, which is separated more than 15° from the center of all the previously defined over-densities. In this way over-density regions are differentiated and isolated. For each of these regions, the midpoint of the highest-density bin will define the corresponding *density peak’s* coordinates.

(iv) We quantify how much a certain satellite s has contributed to a given density peak p (which we refer to as ‘ C_{ps} ’). To this end, we define an aperture angle of 15° around the density peak, selecting all 4-galaxy-normals within it. For each of them, the four contributing satellites are determined. A given satellite s is counted to contribute the 4-galaxy-normal’s *weight* to peak p . Therefore, its final contribution C_{ps} , is the sum of weights corresponding to all the 4-galaxy-normals within the peak aperture that satellite s contributes to. Finally, all satellites are ordered by decreasing C_{ps} to the density peak p , such that the first satellite is that which contributes most.

We note that changing the bin size used in our analysis does not modify our results, as we find the same overdensity regions. While it does slightly change the position found for the density peak centres, the differences are small and do not modify the final order of satellites by C_{ps} . Therefore the final results remain unaltered.

3.2 An extension to the method: plane quality analysis

To allow an individual and in-depth analysis of each overdensity, we present an extension of the 4-galaxy-normal density plot method. Rather than a plane per overdensity, the extension will provide us with a collection of planes with a different number of satellites.

For each over-density p we initially fit a plane to the $N_{\text{sat}}=7$ satellites with highest C_{ps} (i.e., the 7 satellites that contribute most to 4-galaxy-normals within 15° of the density peak), and store the resultant plane parameters. This number $N_{\text{sat}}=7$ is low enough to allow for an analysis of ToI parameter behaviour as N_{sat} increases, and at the same time high enough that we begin with populated planes. Note that taking instead $N_{\text{sat}} = 7 \pm 2$ to begin with does not alter our conclusions.

Then, the next satellite in order of decreasing C_{ps} is added to the group of satellites. Again a plane is fitted to their positions and the parameters stored. This plane-fitting process is repeated until all contributing satellites are used.

To include the effect of distance uncertainties, in practice we calculate 1000 random positions per satellite, and fit 1000 planes at each iteration with N_{sat} satellites. The final results at each N_{sat} correspond to the mean values from these random realizations and the corresponding errors to the standard deviations.

In this way, for each over-density found we obtain a *collection* or catalog of planes of satellites, each plane consisting of an

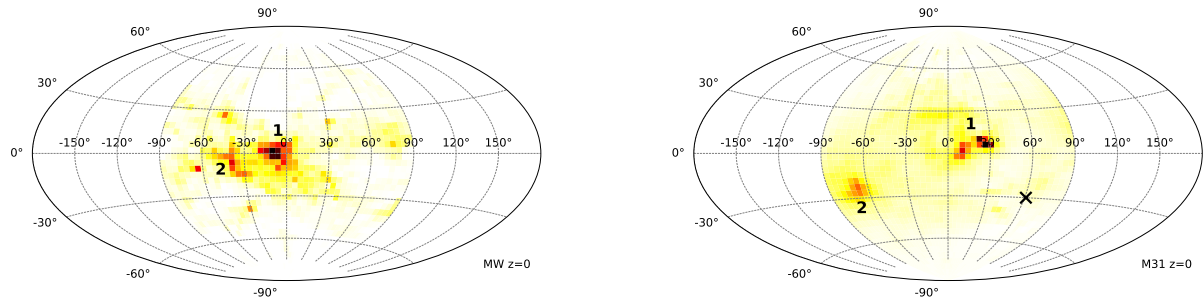


Figure 1. Aitoff projection diagrams of the Milky Way (left) and M31 (right) 4-galaxy-normal density plots (see also Figs. 2 and 4 in Pawlowski et al. 2013). The colormap shows the number of 4-galaxy-normals within a bin, each weighted by $\log\left(\frac{a+b}{c}\right)$ to emphasize planar-like spatial configurations (see Section 3.1 for details). The total number of 4-galaxy-normals is 1755000 for the MW and 4637600 for M31, taking into account 100 random realizations for each (see text). The relevant over-density regions in each map are labeled in order of intensity (Peaks 1 and 2 in the main text). Each diagram is centered on its corresponding central galaxy but the orientation of coordinates in both cases is such that the disc of the MW lies on the latitude $b = 0^\circ$ plane and its spin points along the OZ axis. M31’s spin is marked with an X. A much finer bin size than that shown here has been used to extract the density peak coordinates.

increasing number of members, as well as the quality indicators for each of them.

In this work “high quality” means populated and flattened planes. This is quantified through N_{sat} and c/a (and/or ΔRMS , note that they are very often correlated; see Pawlowski & McGaugh 2014). Being a two-parameter notion, to compare planes’ qualities we need that either N_{sat} is constant or that c/a is constant (or that at least it varies very slowly with N_{sat}). In the first case, lower c/a means higher quality. In the second case, more populated planes are rated as of higher quality. Another case when comparison is possible is when one plane is more flattened and populated than another: the first has a higher quality than the second. These considerations have been applied to the different member planes in the collection obtained for each density peak, allowing us to make quality comparisons, in particular with already determined planes, and, very interestingly, to single out new high-quality ones.⁵

4 RESULTS

Fig. 1 shows Aitoff projection diagrams of the 4-galaxy-normal density plots obtained for the MW and M31 satellite systems. These Aitoff diagrams can be compared to the contour plots in Figs. 2 and 3 from Pawlowski et al. (2013), to which they are essentially identical⁶.

4.1 Milky-Way

As reported in Pawlowski et al. (2013), the MW density plot shows that 4-galaxy-normals are mainly clustered in the region central to the diagram, revealing a planar structure that is polar to the Galaxy (i.e., the normal vector to the plane is perpendicular to the Galaxy’s spin vector). There is one dominant over-density (Peak 1) located

at $(l, b) = (-10.23, 0.41)$, and a second lower density peak (Peak 2) close to the first at $(l, b) = (-39.68, -4.50)$. We will neglect the few isolated bins with intermediate intensity.

Figure 2 shows satellites ordered by contribution to 4-galaxy-normals within 15° around both density peaks (i.e., C_{1s} , upper panel, and C_{2s} , bottom panel). There are 10 satellites that dominate the contribution (i.e., $C_{ps} > 0.5 \times \max(C_{ps}, s = 1, \dots, 27)$), in Peak 1 (i.e., PisII, Car, LeoV, CanVenI, LeoIV, Dra, For, CanVenII, Scl, SexI), while 6 contribute most in Peak 2 (i.e., LeoI, LeoII, CanVenI, CanVenII, For, SexI)⁷. In this case, the contribution is mainly driven by LeoI and LeoII, while the rest of satellites are common with Peak 1 and take low C_{ps} values, indicating the low relevance of this second structure.

4.1.1 Quality analysis

Following our extension to the 4-galaxy-normal method (Section 3.2), for each over-density region we have iteratively computed planes of satellites with an increasing number of members N_{sat} , following the order of satellites given in Fig. 2. In this way, for each peak we obtain an ordered collection of planes, one plane for each N_{sat} . These collections, as well as the identities of the satellites belonging to each plane, can be read out of Figure 2, for both peaks.

The left panel of Fig. 4 shows the results obtained for Peak 1 (solid line) and Peak 2 (dashed line) in the MW. The collection of planes obtained for a given over-density region gives rise to a set of points, with their corresponding error bars, one at each N_{sat} value. They are shown joined with a line, with the corresponding error bands. These are very narrow in the case of the MW, showing that the MW results are not that affected by distance uncertainties.

First we see that, for any N_{sat} value, b/a is rather high (and constant), while c/a is low. Therefore configurations are indeed *planar-like*. Moreover, the lines for both density peaks show rather smooth trends of increasing c/a and ΔRMS with increasing N_{sat} .

⁵ Note that quality as understood in this paper should not be confused with ‘significance’ (meaning the frequency of planes with given characteristics in randomized satellite systems).

⁶ The conversion from the galactocentric longitude convention used here (l) and that used in Pawlowski et al. (2013) (l') is: $l = l' - 180^\circ$.

⁷ Both the location of these peaks and their major contributors are consistent with the results reported in Pawlowski et al. (2013) (see their Fig. 3).

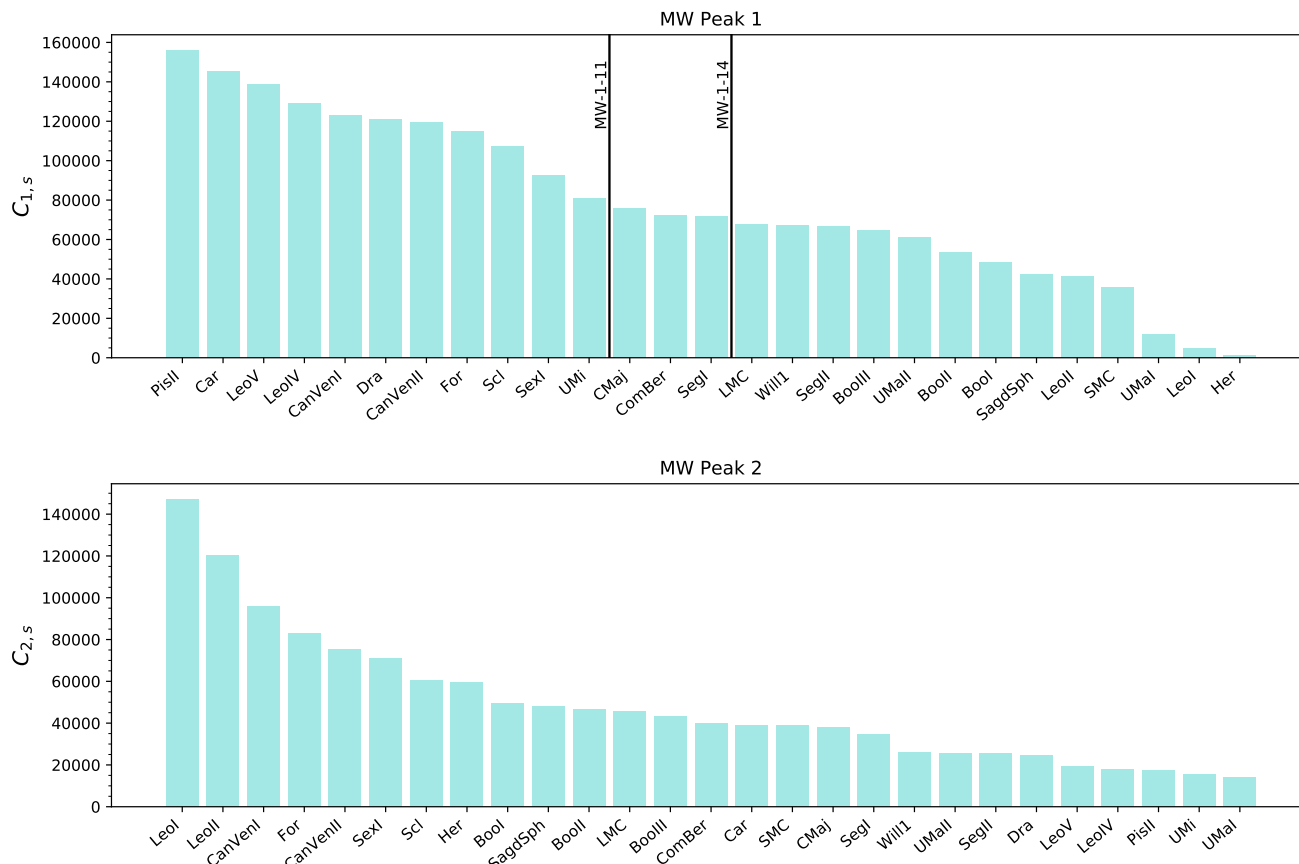


Figure 2. Bar chart showing the contribution of satellites to 4-galaxy-normals in 15° around the first ($C_{1,s}$, top panel) and second ($C_{2,s}$, bottom panel) most important over-densities found in the Milky Way density plot (left panel Fig. 1). The sets of objects that make up the planes of satellites singled out in this work are delimited with vertical lines and labeled correspondingly (see Tab 2).

In particular, the MW Peak 1 line defines a planar structure of satellites with a higher quality (i.e., lower c/a , lower ΔRMS at given N_{sat}), than that defined by Peak 2. This is expected, given the higher density of 4-galaxy-normals in Peak 1 than in Peak 2 (see Fig. 1). This suggests that the MW satellite sample seems to be a unique highly planar-like organized structure, as we had already learnt from Fig. 2. We also note that both the c/a and ΔRMS versus N_{sat} curves roughly show the same shape patterns, due to the lack of significant b/a variation as N_{sat} increases. Therefore, including ΔRMS on top of c/a in the quality analysis generally does not add any relevant information.

In the bottom panels we give the directions of the normal vectors corresponding to the best fitting planes (obtained from the satellites' most-likely positions) as a function of N_{sat} . Shaded regions show the corresponding spherical standard distances Δ_{sph} (Metz et al. 2007), a measure of the planes normals' collimation for the 1000 realizations. The normal directions to planes from both Peak 1 and 2 in the MW remain very stable as N_{sat} increases, and their uncertainties due to satellite distance errors are very small.

As for the plane distances to the MW, D_{cg} is below 16 kpc in all plane-fitting iterations in Peak 1, and below 12.5 kpc in the case of Peak 2.

For reference, overplotted colored points show the values on this diagram for the observed planes of MW satellites mentioned in the literature (classical, VPOS-3, VPOSall; see Table 1), defined

from Peak 1 (Pawlowski et al. 2013). We note that the points corresponding to the VPOS-3 and VPOSall planes fall over the trend given by the solid line, as expected. On the other hand, and very interestingly, this analysis shows that there is a different combination of $N_{\text{sat}}=11$ satellites that results in a much flatter and thinner plane than the classical one (see MW-1-11⁸ in Table 2). In fact, the plane including $N_{\text{sat}}=14$ satellites (MW-1-14 in Table 2) presents an even higher quality than that with $N_{\text{sat}}=11$, as c/a remains roughly constant at a higher N_{sat} .

This is possible because this analysis uses the 3-dimensional information of positions, while the classical plane of satellites was found observationally when only the most luminous (i.e. massive) satellites were known to exist. This important result indicates that planes of satellites are not necessarily composed by the most massive satellites of a galactic system (see also Libeskind et al. 2005; Collins et al. 2015) and hence they should not be searched for in this way. Indeed, we find that M_{star}^9 is not correlated with $C_{1,s}$ (contribution to the main over-density region, where we find the highest quality planes): the correlation coefficient r is low, in such

⁸ Planes underlined in this work, either for the MW or M31, are named after the peak where they have been identified and the number of satellites they include (i.e., [Host-Peak- N_{sat}]).

⁹ Observational stellar masses have been computed applying the Woo et al. (2008) mass-to-light ratios to the luminosities in McConnachie (2012).

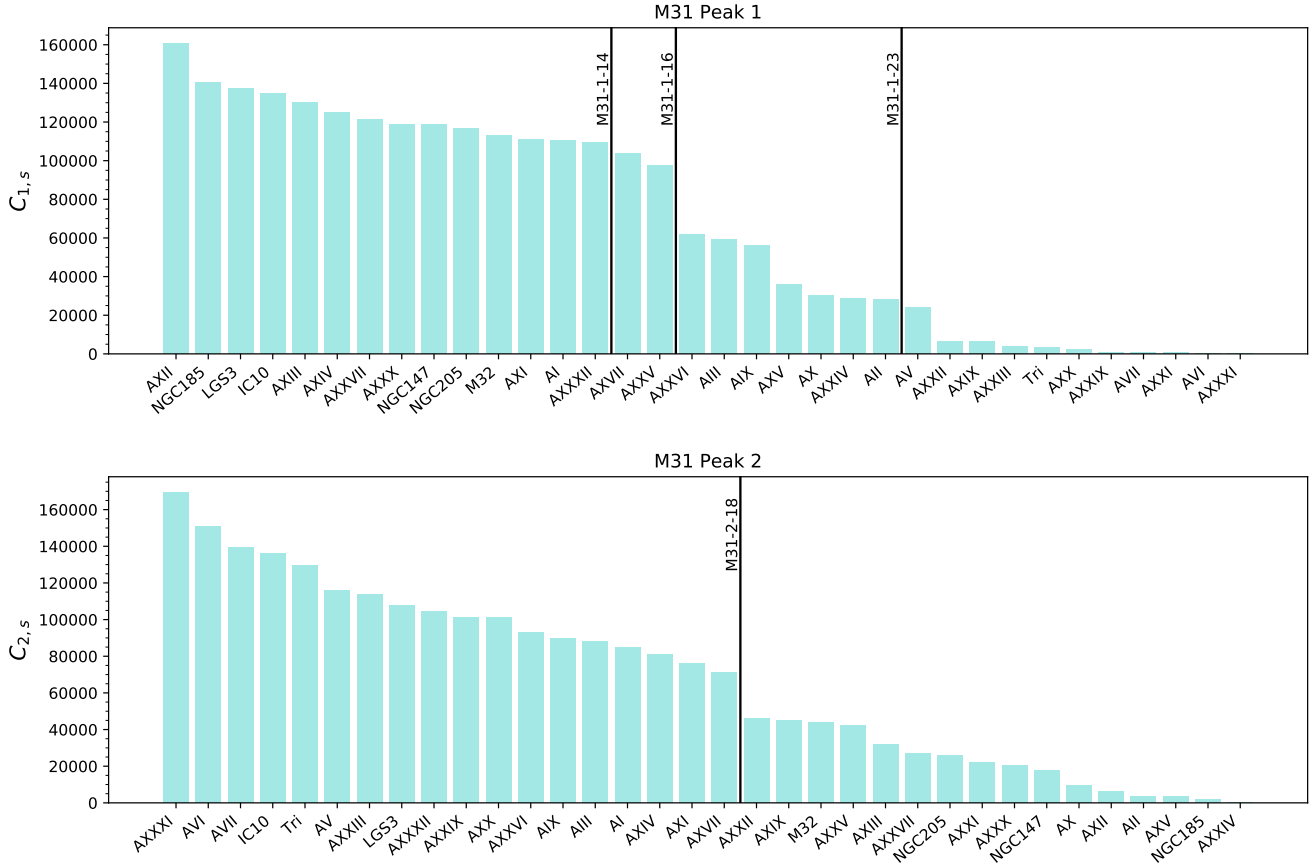


Figure 3. Same as Fig. 2 for M31. Both the first (top panel) and second (bottom panel) over-densities of M31’s 4-galaxy-normal density plot have similar intensities which is reflected in a high and comparable contribution from satellites in both bar charts.

a way that the probability of getting such value assuming that there is no correlation is higher than 76% (see upper panel in Fig. 5).

4.2 Andromeda M31

Figure 1 reveals, as in the MW, two 4-galaxy-normal over-densities in M31. In this case they both show high, comparable intensities and are located quite separate ($\sim 80^\circ$) from one another. We define Peak 1 as the over-density at $(l, b) = (26.60, 6.14)$, and Peak 2 as that located at $(l, b) = (-69.14, -21.68)$. The direction of M31’s spin vector, depicted with an ‘X’, indicates that the planar configurations defined by both peaks are not perpendicular to the galaxy’s disc, but inclined 48.93° and 70.49° , respectively. Interestingly, Peak 1 forms an angle of 83.86° with the MW’s spin vector, meaning its corresponding planes are approximately normal to the MW’s disc (Conn et al. 2013). Furthermore, the projected angular distance on the sphere between Peak 1 and Peak 2 is of 82.43° , and the angle between Peak 1 (Peak 2) and the Sun - M31 line is 87.73° (5.31°). Therefore the planar configuration of satellites defined by Peak 1 is observed nearly edge-on from the MW (see also Pawlowski et al. 2013 Table 5), while that of Peak 2 is approximately perpendicular to it and would be observed mostly face-on.

Fig. 3 shows that approximately half of the satellite sample contributes dominantly to each corresponding peak p . Focusing on the identities of satellites, we find that, out of the 16 satellites with highest $C_{1,s}$, 9 are among the satellites with lowest $C_{2,s}$. On

the other hand, out of the 17 satellites with highest $C_{2,s}$, 10 are among those with lowest $C_{1,s}$. This is indicating that the two over-densities’ contributing members are not the same. While satellites contributing most to Peak 1 define the GPoA plane from Pawlowski et al. (2013) (and also generally coincide with satellites in “plane 1” from Shaya & Tully (2013)), Peak 2 and its corresponding predominant planar satellite configuration have not been analyzed prior to this study¹⁰ and will be described in detail below.

4.2.1 Quality analysis

For each peak, we build up their respective collections of planes of satellites by iteratively applying the best-fitting plane technique to an increasing number of satellites N_{sat} following the order given by Fig. 3. The values of concentration ellipsoid parameters versus N_{sat} are shown in the right panel of Fig. 4. We see that c/a and b/a take respectively low and high values, confirming that these spatial distributions are actually planes up to $N_{\text{sat}} \sim 24-25$. When considering the whole sample of M31 satellites, c/a and b/a take a similar value of ~ 0.6 , indicating instead a non-flattened ellipsoidal spatial distribution.

¹⁰ Note that the planar structure derived here from Peak 2 does not correspond to the so-called ‘M31 disc plane’ noted in Pawlowski et al. (2013), or to “plane 2” in Shaya & Tully (2013).

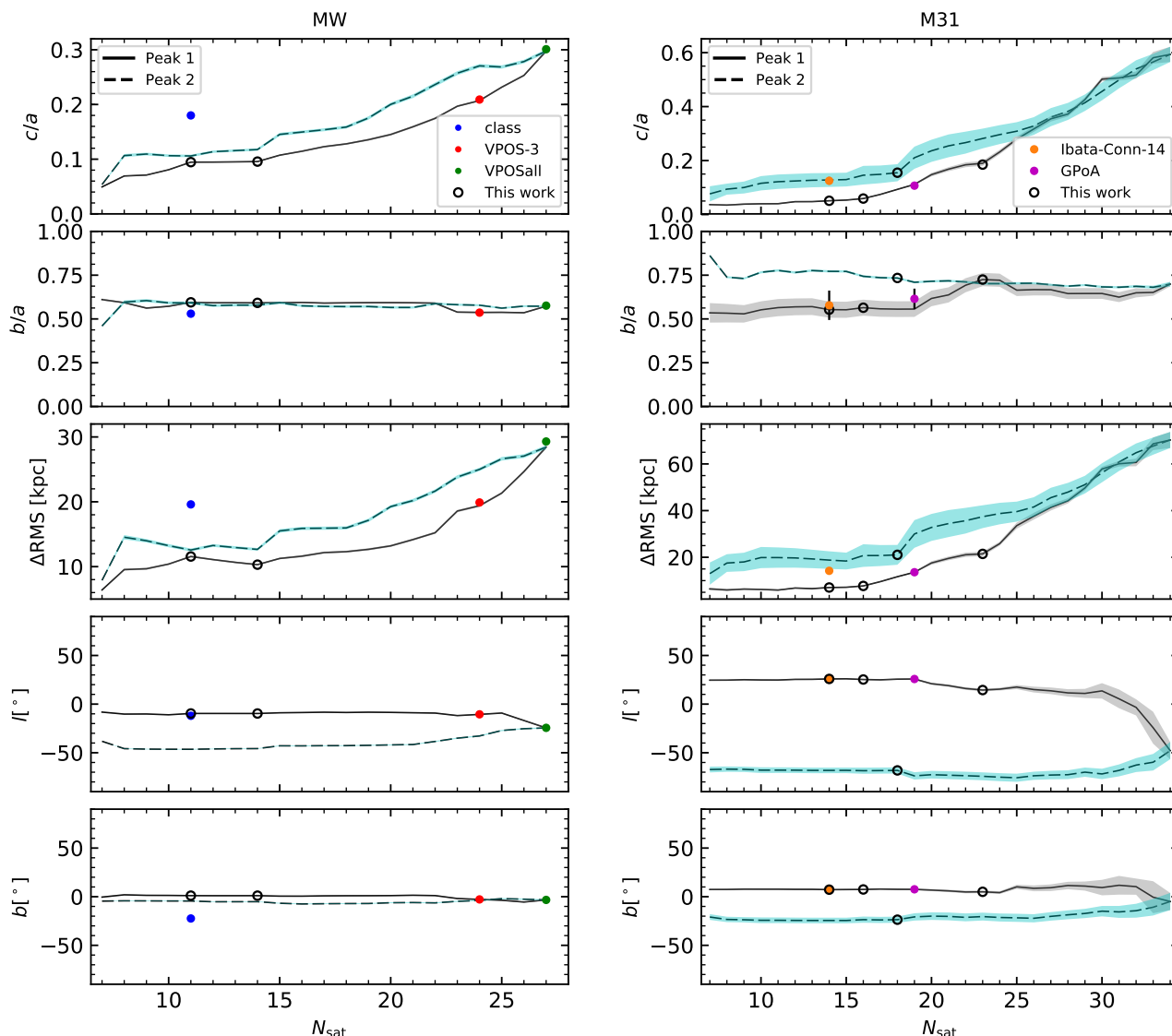


Figure 4. Quality analysis of the main planar structures found in the Milky Way (left panels) and in M31 (right panels) with the 4-galaxy-normal density plot method (see Figs. 1). Lines show c/a , b/a , ΔRMS and the direction of normal vectors to the best-fitting plane (l , b) as a function of N_{sat} . Except in the l or b versus N_{sat} panels, results are the mean values of 1000 realizations at each N_{sat} , and shaded regions show the standard deviations. (l , b) directions have been calculated using the most-likely positions of satellites and shaded regions show the corresponding uncertainties in terms of the spherical standard distance Δ_{sph} (Metz et al. 2007). As expected, the two curves in each panel converge for the maximum N_{sat} since the samples of satellites become identical. Colored circles show the results for the reported observed planes of satellites in the MW (classical, VPOS-3, VPOSall), and in M31 (‘Ibata-Conn-13’ and GPoA), respectively. Their specific values including their errors are given in Table 1. The planes of satellites singled out in this work are shown with black open circles, and their corresponding ToI parameters are given in Table 2.

The corresponding parameter error bands are clearly apparent in the case of M31 as compared to the MW, due to overall larger satellite distance uncertainties. As mentioned previously, while the GPoA is viewed approximately edge-on from the Sun, the planes of satellites from Peak 2 are viewed mostly face-on. Therefore the uncertainties in the Sun - satellite distances affect more (less) to the c/a and ΔRMS parameters than to b/a , in the case of Peak 2 (Peak 1). This fact explains the different magnitude of the error bands among the ToI parameters shown in this figure.

Focusing on the c/a and ΔRMS panels, one can see that only up to \sim half of the total number of satellites contributing respectively to Peak 1 and Peak 2 form a thin planar structure, which rapidly thickens as more members are added to the plane-fitting iteration. Moreover, as said above, satellite identities contributing

most to both peaks are overall different as shown in Fig. 3. Therefore, in contrast to the MW, the M31 satellite sample does not form one preferential planar structure but seems to be divided in (at least) two.

The normal directions to the planes are stable as N_{sat} increases and reaches $N_{\text{sat}} = 19$ for Peak 1 and $N_{\text{sat}} = 18$ for Peak 2, showing that the two satellite planar structures are well defined. Beyond these values, the normals to the corresponding planes are not that well fixed.

As for the distances, planes around Peak 1 pass close to the M31 center, while planes belonging to Peak 2 do not (see values in Tab. 2). Their distances are large but still within reasonable ranges to allow for the possibility of dynamical stability in a complex, binary system like the Local Group, especially if we take into account

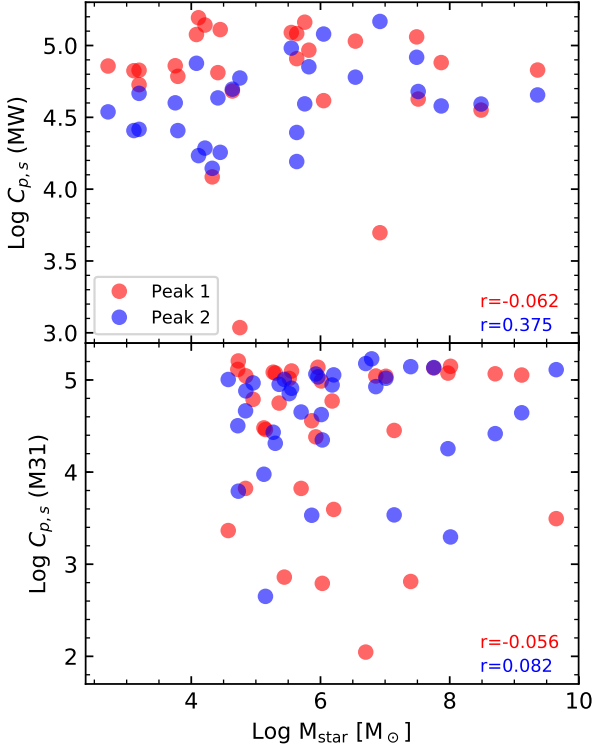


Figure 5. The contribution of satellites to 4-galaxy-normals within 15° of the main density peaks, $C_{p,s}$, versus stellar mass. The Pearson correlation coefficients r are given in each case.

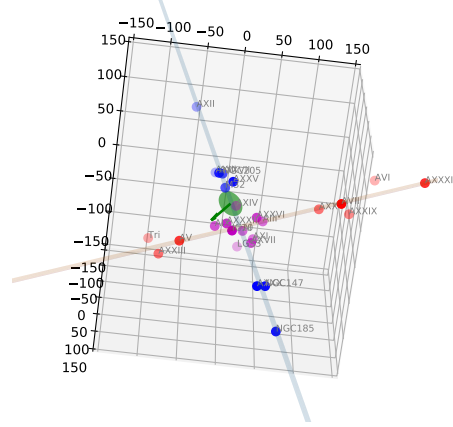
the large distance uncertainties (see errors in Tab. 2) and consider the important lopsidedness in the distribution of M31 satellites (see [McConnachie & Irwin 2006](#); [Ibata et al. 2013](#)).

The specific values for M31 Ibata-Conn-14 and GPoA planes are shown with colored circles in Fig. 4 (see Table 1). Our methodology reveals a combination of $N_{\text{sat}} = 14$ satellites (marked with a black open circle in Fig. 4, right panels) that yields a higher quality plane than the ‘Ibata-Conn-14’ plane (see M31-1-14 entry in Table 2 and Fig. 3 for satellite identities). This occurs because the ‘Ibata-Conn-14’ plane was defined among only PAndAS survey satellites, while the sample used in [Pawlowski et al. \(2013\)](#) and here includes the PAndAS satellites within 300 kpc of M31 (25 out of 27) plus 9 satellites discovered differently (i.e., LGS3, IC10, AXXXII, AVII, AXXXI, AVI, NGC205, M32). Interestingly, the latter turn out to be precisely among the dominant 4-galaxy-normal contributors to both M31 Peaks 1 and 2.

In turn, the magenta circles corresponding to the GPoA match the solid line (Peak 1) because the 19 satellites that we find with highest C_{1s} are precisely the GPoA satellite sample. Note that the satellite system shows low correlation coefficients r between M_{star} and C_{1s} or C_{2s} , with a higher than 75% probability of getting such r values assuming that there is no correlation (see lower panel of Fig. 5).

Moreover, our analysis allows the identification of the highest quality planes in M31 as N_{sat} increases at c/a roughly constant. These planes correspond to the points in Fig. 4 at which the M31 Peak 1 and Peak 2 lines start to increase rapidly in the c/a and ΔRMS panels, marked in Fig. 4 with black open circles. For Peak

Figure 6. Edge-on view of M31-2-18, the highest-quality plane from Peak 2 in M31 with $N_{\text{sat}}=18$ members (in red), and the GPoA (in blue), showing their relative orientation. M31’s galactic disc and spin vector are depicted in green. Satellites belonging only to the M31-2-18 plane are shown as red points, while satellites belonging only to the GPoA are shown as blue points. Satellites shared by both samples are violet.



1 the highest quality plane at low c/a occurs with $N_{\text{sat}}=16$ (M31-1-16 in Table 2) and for Peak 2, with $N_{\text{sat}}=18$ members (M31-2-18), beyond which the normal vector $\vec{n}(l, b)$ to the best-fitting plane does not conserve its direction. The latter presents comparable properties to the GPoA (magenta circle), to which it is roughly perpendicular. Indeed, given that the GPoA has one satellite more and a lower c/a value than the M31-2-18 plane (see Tabs. 1 and 2), strictly speaking the former has a higher quality than the latter. However, the differences are a 5% in N_{sat} , and a 10% in the c/a values, taking into account the error bars. Therefore we can conclude that the qualities of both planes are comparable.

Figure 6 shows the relative orientation between M31-2-18 and the GPoA. Note that 10 satellites are shared by both samples (i.e., LGS3, IC10, AXIV, AXI, AXXXII, AI, AXVII, AIX, AIII and AXXVI, in violet in the figure).

It is of interest whether this plane could be dynamically stable, this is, if the member satellites corotate within the planar structure they define in space. Line-of-sight velocities of the M31-2-18 satellites (taken from [McConnachie 2012](#); [Collins et al. 2013](#); [Martin et al. 2014](#)), which we observe face-on from the MW, give a perpendicular velocity dispersion of $\sigma = 90.20$ km/s. According to [Fernando et al. \(2017\)](#), such a plane will be erased in a short timescale and is just a fortuitous alignment of satellites, as they find that planes with a perpendicular velocity dispersion above ~ 50 km/s disperse to contain half their initial number of satellites in 2 Gyrs time.

Finally, we also note the high quality of the plane with $N_{\text{sat}}=23$ from Peak 1 (M31-1-23 in Table 2), with ToI parameter values very similar to those of the VPOS-3 plane of satellites in the MW.

5 SUMMARY AND CONCLUSIONS

Recent studies on planes of satellites have resorted to evermore refined methods to define and characterize them. In this work, we have further developed one such method, the ‘4-galaxy-normal density plots’ method ([Pawlowski et al. 2013](#)), with an extension designed to identify, systematically catalog and study in detail the

quality of the predominant planar configurations revealed by over-densities in the 4-galaxy-normal density plots.

We count the weighted number of times each satellite s contributes to 4-galaxy-normals within 15° of a specific over-density p (C_{ps}). For each relevant over-density, we order satellites by decreasing C_{ps} and iteratively fit planes to subsamples of satellites following this order. In this way, rather than a plane per over-density, we yield a catalog or *collection of planes* of satellites with an increasing number of members N_{sat} , whose normals cluster around the density peak.

The quality of planes is quantified through the number of member satellites N_{sat} and the degree of flattening. The latter is measured through the short-to-long axis ratio of the Tensor of Inertia (ToI, Metz et al. 2007) concentration ellipsoid, c/a (and/or the r.m.s thickness normal to the plane, ΔRMS , which are often correlated), provided there is a high intermediate-to-long axis ratio, b/a , which confirms a planar-like spatial distribution of satellites. Quality comparisons between planes are done either considering constant N_{sat} (where a lower c/a means higher quality) or constant c/a (where more populated planes have higher quality). In this way, we are able to single out new high-quality planes.

This method has been applied to the positional data of MW and M31 confirmed satellites (McConnachie 2012; Pawlowski et al. 2013). Two predominant, collimated over-density regions show up in each of their respective 4-galaxy-normal density plots. They reveal that both satellite samples are highly structured in planar-like configurations. However, they show very different patterns: while satellites in the MW form basically one main polar structure, M31 satellites are spatially distributed along *two* distinct collections of planes, inclined with respect to the M31 disc and roughly perpendicular to each other.

We find planes of satellites with higher qualities than those previously reported with a given N_{sat} . More specifically, we find a combination of 11 MW satellites that spatially describe a plane with much higher quality than that defined by the 11 classical (the most massive) satellites. Similarly for M31, we present a combination of 14 satellites with much lower c/a and ΔRMS values than those of the plane noted by Ibata et al. (2013) and Conn et al. (2013) (Ibata-Conn-14 plane) with the PAndAS survey.

For the first time, the second-most predominant planar structure (Peak 2) found in M31 has been studied in detail (Peak 1 was studied in Pawlowski et al. (2013)). This peak points to a satellite planar configuration whose normal direction aligns with the line-of-sight between the Sun and M31, and therefore is viewed nearly face-on (we recall that the planar configuration defined by M31 Peak 1 –containing the well-known GPoA with $N_{\text{sat}}=19$ – is viewed nearly edge-on). Our analysis reveals a rich plane structure, with quality behaviour in terms of c/a and ΔRMS versus N_{sat} similar to that found around Peak 1, despite being more affected by the radial Sun - satellite distance uncertainties due to its orientation. The satellites contributing to this second planar configuration have overall a different identity than those contributing to Peak 1.

In particular, both c/a and ΔRMS increase sharply for $N_{\text{sat}} > 16$ satellites around Peak 1, and for $N_{\text{sat}} > 18$ around Peak 2. Therefore we state that the planes of satellites with precisely these N_{sat} values represent the *highest quality* planar structures for each peak, among the confirmed satellites within 300 kpc of M31. As evidence, the planes' normals stay stable up to $N_{\text{sat}} = 19$ for Peak 1, and $N_{\text{sat}} = 18$ for Peak 2, and then they change. Interestingly, the plane from Peak 1 with $N_{\text{sat}}=16$ is more populated and thinner than the Ibata-Conn-14 plane. Moreover, the plane with $N_{\text{sat}}=18$ from Peak 2 presents very similar properties to

the GPoA but consists of an overall different satellite sample. This plane of satellites had not been informed for so far.

Finally, the richer plane structure in the MW and M31 we report in this work was found because we allow the mass of satellites to play no role in our search. Indeed, through correlation tests we find that mass is not a satellite property that determines its 4-galaxy-normal contribution to the main over-density regions (i.e., its membership or not to the respective best-quality planes), either in the MW or M31 cases. This is expected, given that globular clusters and streams have been found to align as well with the VPOS (Pawlowski et al. 2012).

ACKNOWLEDGEMENTS

This work was supported through MINECO/FEDER (Spain) AYA2012-31101, AYA2015-63810-P and MICIIN/FEDER (Spain) PGC2018-094975-C21 grants. ISS acknowledges funding from the European Union's Horizon 2020 research and innovation programme under the Marie Skłodowska-Curie grant agreement No. 734374 (LACEGAL-RISE) for a secondment at the Astrophysics group of Univ. Andrés Bello (Santiago, Chile), and from the Univ. Autónoma de Madrid for a stay at the Leibniz Institut für Astrophysik Potsdam (Germany). She thanks Dr. Patricia Tissera and Dr. Noam Libeskind for kindly hosting her.

REFERENCES

- Bechtol K. et al., 2015, ApJ, 807, 50
 Collins M. L. M. et al., 2013, ApJ, 768, 172
 Collins M. L. M. et al., 2015, ApJ, 799, L13
 Conn A. R. et al., 2013, ApJ, 766, 120
 CRAMR H., 1999, Mathematical Methods of Statistics (PMS-9). Princeton University Press
 Fernando N., Arias V., Guglielmo M., Lewis G. F., Ibata R. A., Power C., 2017, MNRAS, 465, 641
 Fritz T. K., Battaglia G., Pawlowski M. S., Kallivayalil N., van der Marel R., Sohn T. S., Brook C., Besla G., 2018, ArXiv e-prints, arXiv:1805.00908
 Fusi Pecci F., Bellazzini M., Cacciari C., Ferraro F. R., 1995, AJ, 110, 1664
 Gaia Collaboration et al., 2018, A&A, 616, A12
 Grebel E. K., Kolatt T., Brandner W., 1999, in IAU Symposium, Vol. 192, The Stellar Content of Local Group Galaxies, White-lock P., Cannon R., eds., p. 447
 Ibata R. A. et al., 2013, Nature, 493, 62
 Keller S. C., Mackey D., Da Costa G. S., 2012, ApJ, 744, 57
 Koch A., Grebel E. K., 2006, AJ, 131, 1405
 Koposov S. E., Belokurov V., Torrealba G., Evans N. W., 2015, ApJ, 805, 130
 Kroupa P. et al., 2010, A&A, 523, A32
 Kroupa P., Theis C., Boily C. M., 2005, A&A, 431, 517
 Kunkel W. E., Demers S., 1976, in The Galaxy and the Local Group, Vol. 182, p. 241
 Libeskind N. I., Frenk C. S., Cole S., Helly J. C., Jenkins A., Navarro J. F., Power C., 2005, MNRAS, 363, 146
 Lynden-Bell D., 1976, MNRAS, 174, 695
 Lynden-Bell D., 1982, The Observatory, 102, 202
 Majewski S. R., 1994, ApJ, 431, L17
 Martin N. F. et al., 2014, ApJ, 793, L14
 Martin N. F. et al., 2016, ApJ, 833, 167

Table 1. ToI fitting properties of the observed planes of satellites in the MW (classical, VPOSall, VPOS-3) and M31 (Ibata-Conn-14, GPoA): Galactic coordinates of the normal to the plane; uncertainty in the normal direction; distance to the MW/M31; root-mean-square height of the plane; short-to-long ellipsoid axis ratio; intermediate-to-long ellipsoid axis ratio; number of satellites included in the plane. Information for the classical plane of MW satellites has been taken from Metz et al. (2007) and Pawlowski (2016). The information for all rest of planes has been extracted from Pawlowski et al. (2013) (see their Table 3), where distance uncertainties are considered by sampling the distances 1000 times with a Gaussian distribution around their most-likely distance.

Name	MW			M31	
	classical	VPOSall	VPOS-3	Ibata-Conn-14	GPoA
$\vec{n}(l, b)$ [°]	(-22.7, -12.7)	(-24.4, -3.3)	(-10.5, -2.8)	(26.2, 7.8)	(25.8, 7.6)
$\Delta_{\text{sph}} n$ [°]	–	1.12	0.43	1.00	0.79
D_{MW} [kpc]	8.3	7.9 ± 0.3	10.4 ± 0.2	–	30.1 ± 8.8
D_{M31} [kpc]	–	637.3 ± 13.0	509.9 ± 10.2	4.1 ± 0.7	1.3 ± 0.6
$\Delta\text{RMS height}$ [kpc]	19.6	29.3 ± 0.4	19.9 ± 0.3	14.2 ± 0.2	13.6 ± 0.2
c/a	0.18	0.301 ± 0.004	0.209 ± 0.002	0.125 ± 0.014	0.107 ± 0.005
b/a	0.53	0.576 ± 0.007	0.536 ± 0.006	0.578 ± 0.084	0.615 ± 0.058
N_{sat}	11	27	24	14	19

Table 2. Same as Table 1 for the high quality planes singled out in this work.

Name	[Host-Peak- N_{sat}]					
	MW-1-11	MW-1-14	M31-1-14	M31-1-16	M31-1-23	M31-2-18
$\vec{n}(l, b)$ [°]	(-9.6, 1.1)	(-9.7, 1.1)	(25.9, 7.2)	(25.3, 7.4)	(14.4, 5.0)	(-68.2, -23.6)
$\Delta_{\text{sph}} n$ [°]	0.15	0.15	0.45	0.51	1.40	3.16
D_{MW} [kpc]	15.0 ± 0.1	14.6 ± 1.0	36.2 ± 4.9	40.9 ± 5.8	185.7 ± 15.0	741.6 ± 6.5
D_{M31} [kpc]	464.5 ± 6.3	465.2 ± 6.3	1.1 ± 0.4	0.6 ± 0.5	2.3 ± 1.8	34.9 ± 11.2
$\Delta\text{RMS height}$ [kpc]	11.6 ± 0.1	10.3 ± 0.1	7.0 ± 0.2	7.7 ± 0.2	21.4 ± 1.0	21.0 ± 4.2
c/a	0.095 ± 0.001	0.096 ± 0.001	0.051 ± 0.002	0.059 ± 0.002	0.189 ± 0.009	0.155 ± 0.032
b/a	0.595 ± 0.004	0.592 ± 0.004	0.553 ± 0.046	0.564 ± 0.046	0.725 ± 0.038	0.734 ± 0.006
N_{sat}	11	14	14	16	23	18

- Martínez-Delgado D., Butler D. J., Rix H.-W., Franco V. I., Peñarrubia J., Alfaro E. J., Dinescu D. I., 2005, *ApJ*, 633, 205
 Mateu C., Vivas A. K., Zinn R., Miller L. R., Abad C., 2009, *AJ*, 137, 4412
 McConnachie A. W., 2012, *AJ*, 144, 4
 McConnachie A. W., Irwin M. J., 2006, *MNRAS*, 365, 902
 McConnachie A. W. et al., 2009, *Nature*, 461, 66
 Metz M., Kroupa P., Jerjen H., 2007, *MNRAS*, 374, 1125
 Metz M., Kroupa P., Jerjen H., 2009, *MNRAS*, 394, 2223
 Momany Y., Zaggia S. R., Bonifacio P., Piotto G., De Angeli F., Bedin L. R., Carraro G., 2004, *A&A*, 421, L29
 Müller O., Jerjen H., Pawlowski M. S., Binggeli B., 2016, *A&A*, 595, A119
 Müller O., Pawlowski M. S., Jerjen H., Lelli F., 2018, *Science*, 359, 534
 Pawlowski M. S., 2016, *MNRAS*, 456, 448
 Pawlowski M. S., Kroupa P., 2014, *ApJ*, 790, 74
 Pawlowski M. S., Kroupa P., Jerjen H., 2013, *MNRAS*, 435, 1928
 Pawlowski M. S., McGaugh S. S., 2014, *ApJ*, 789, L24
 Pawlowski M. S., McGaugh S. S., Jerjen H., 2015, *MNRAS*, 453, 1047
 Pawlowski M. S., Pflamm-Altenburg J., Kroupa P., 2012, *MNRAS*, 423, 1109
 Shaya E. J., Tully R. B., 2013, *MNRAS*, 436, 2096
 Tully R. B., Libeskind N. I., Karachentsev I. D., Karachentseva V. E., Rizzi L., Shaya E. J., 2015, *ApJ*, 802, L25
 Woo J., Courteau S., Dekel A., 2008, *MNRAS*, 390, 1453
 York D. G. et al., 2000, *AJ*, 120, 1579